Accepted Manuscript

Characterization and thermal performance evaluation of infrared reflective coatings compatible with historic buildings

Francesca Becherini, Elena Lucchi, Alessandra Gandini, Maria Casado Barrasa, Alexandra Troi, Francesca Roberti, Maria Sachini, Maria Concetta Di Tuccio, Leire Garmendia Arrieta, Luc Pockelé, Adriana Bernardi

PII: S0360-1323(18)30106-9

DOI: 10.1016/j.buildenv.2018.02.034

Reference: BAE 5318

To appear in: *Building and Environment*

Received Date: 14 December 2017

Revised Date: 21 February 2018

Accepted Date: 22 February 2018

Please cite this article as: Becherini F, Lucchi E, Gandini A, Barrasa MC, Troi A, Roberti F, Sachini M, Di Tuccio MC, Arrieta LG, Pockelé L, Bernardi A, Characterization and thermal performance evaluation of infrared reflective coatings compatible with historic buildings, *Building and Environment* (2018), doi: 10.1016/j.buildenv.2018.02.034.

TITLE

CHARACTERIZATION AND THERMAL PERFORMANCE EVALUATION OF INFRARED REFLECTIVE COATINGS COMPATIBLE WITH HISTORIC BUILDINGS

Authors:

Francesca Becherini[1], Elena Lucchi[2,*], Alessandra Gandini[3], Maria Casado Barrasa[4], Alexandra Troi[2], Francesca Roberti[2], Maria Sachini[5], Maria Concetta Di Tuccio[1], Leire Garmendia Arrieta[6], Luc Pockelé[7], Adriana Bernardi[1]

[1]: Institute of Atmospheric Sciences and Climate, National Research Council, Italy
[2]: EURAC Research, Italy
[3]: TECNALIA, Sustainable Construction, Spain
[4]: ACCIONA Construccion S.A., Technology Centre, Alcobendas, Spain
[5]: AMSolutions, Greece
[6]: Department of Mechanical Engineering, University of the Basque Country UPV/EHU, Bilbao, Spain
[7]: R.E.D. srl, Italy
* corresponding author (e-mail: elena.lucchi@eurac.edu; Tel: +39 0471 055 653)

Keywords: Envelope retrofitting; Reflective coating; Historic Buildings; Thermal performance; Reversibility

ABSTRACT

Two infrared reflective coatings recently developed as part of the EFFESUS European research project are characterized and evaluated in this paper. Thermal performance, durability, compatibility with historic fabric, and reversibility are all analysed. The results of extensive research that include laboratory analysis of selected substrates, measurements on a large-scale traditional masonry mock-up, thermodynamic simulations, and finally application in to a real historic building in Istanbul, all support the potential of the new coatings to improve the thermal performance of historic buildings, in keeping with their visual integrity and cultural value. Besides their reflective properties, proven by the thermal stress reductions on the treated surfaces, the new coatings are characterized by low visual impact, easy application, material compatibility, and reversibility after application, as well as durability over time.

1. INTRODUCTION

Reflective coatings are passive solutions that reflect a proportion of incidental infrared (IR) surface radiation. They contribute to mitigation of the effects of the heat island phenomenon at an urban level, while decreasing the cooling demand in summer and improving indoor thermal comfort within the building. The literature contains immense scientific effort to design geo-engineering solutions for the effective mitigation of climate change and the consequent heat island effect, using high albedo materials for “cool roofs”, urban paving and building envelopes [1]. The development and the environmental and energetic performance of cool coatings technologies are widely discussed in two review articles [2; 1]. The first generation of cool coatings consisted of natural materials (generally, natural stone aggregates) with a high albedo (higher than 0.8), light colours and walkable surfaces for application principally on roofs and pavements [1; 3; 4]. Then, a second generation of non-white materials with an albedo higher than the first generation of coatings was also recently

developed for use on historical roofs and façades [1]. These materials are characterized by higher albedo and reflectance levels within the non-visible region of the solar spectrum (generally near IR) than conventional coloured coatings with the consequent reduction of their surface temperature (T_s) when exposed to solar radiation [1; 5].

Literature reviews have demonstrated that the reduction of T_s and the urban heat island effects of a coating depend on a variety of complex factors [1; 6]: (i) geomorphology of the territory; (ii) design of urban layout and vegetation; (iii) anthropogenic heat intensity; (iv) local weather conditions; (v) orientation; (vi) characteristics of urban built environments and building skins; and, (vii) difference between exterior and interior T_s. In general, the benefits of these coatings applied to building envelope (roofs and façades) concern the reduction of T_s [7], energy needs [8], and cooling loads and CO_2 equivalent emissions for cooling associated with HVAC operation [9; 10], as well as the improvement of the indoor thermal comfort conditions in summer [11]. In addition, the experimental studies and numerical analyses of the energy performance of IR coatings identified a potential balance between summer benefits and winter penalties related to the coating application on the building envelope (façades [12] and cool roofs [11]) in different climatic conditions. Therefore, appropriate design and application and adequate experimental testing are crucial to assess their thermal performance [1; 13; 14].

The literature also contains examples in which the development and the performance optimization of new IR coatings are supported by laboratory measurements, computer simulations and field testing [1; 8; 6; 9; 10; 11; 12]. Despite the high effectiveness of these coatings in terms of energy efficiency in a wide range of building applications, the existing commercial products are not normally suitable for historic fabric, where the intervention requires an integral blend with the original building elements, hence low visual and architectonic impact [15].

Cultural heritage needs to be preserved for future generations and the application and subsequent removal of any treatment should not leave a building undamaged [16]. Innovative commercial products usually have the same appearance as traditional tiles and mainly consist of cool clay tiles with high solar reflectance (0.75), because of the high thermal emissivity (ε), and chemical-physical durability of ceramic products [1]. Even so, the paintings and coatings developed for application on cool roofs in particular were not compatible with heritage buildings [1].

In this context, the development and the testing of the new coatings are specific tasks of the EFFESUS European research project (***E**nergy e**FF**iciency for **E**U Historic Districts' **SU**stainability*). The coatings are compatible with historic materials, capable of reducing the absorption of IR radiation on building surfaces, and of decreasing energy consumption for cooling in summer, with no intrusive impact on the building fabric. Besides possessing highly reflective properties, the coatings have to meet specific requirements for application on historic buildings (i.e. physical-chemical compatibility, durability, reversibility, and low visual impact). The two novel IR reflective coating formulations compatible with historic building materials are characterized in this study. Laboratory tests and building energy simulation were conducted, to evaluate and to maximize the performance of the two formulations. Finally, their behaviour was tested on an historic building under the climatic conditions in Istanbul, Turkey.

2. MATERIAL AND METHODS

In order to gain two major objectives of the experimental work: i) to verify the applicability and compatibility of the developed IR coatings with cultural heritage and ii) to identify the most suitable and better performing one in terms of thermal performance (temperature reduction), compatibility with cultural heritage (or Reversibility and aesthetic impact) and

durability, the following steps were planned and described in detail in the following subsections:

1. Selection and characterization of the substrates commonly used in European cultural heritage buildings;
2. Development and application of two IR reflective coatings on the selected substrates;
3. Substrate physical-chemical characterization after coatings application;
4. Reversibility and visual impact;
5. Durability tests at laboratory scale;
6. Thermal performance evaluation of one coating on a large scale mock-up wall;
7. Thermodynamic simulation of the same coating in a reference room to evaluate its energy and thermal performance;
8. Application of the two coatings under real conditions and evaluation of their thermal performance, durability, and reversibility.

2.1 Selection and characterization of substrates

The following four substrates were considered representative of the materials most commonly used in cultural heritage buildings in Europe in terms of porosity and pore size distribution: (a) Villamayor Sandstone; (b) Istanbul stone (the same used in the Istanbul case study); (c) solid clay bricks; and, (d) lime mortar (Figure 1).

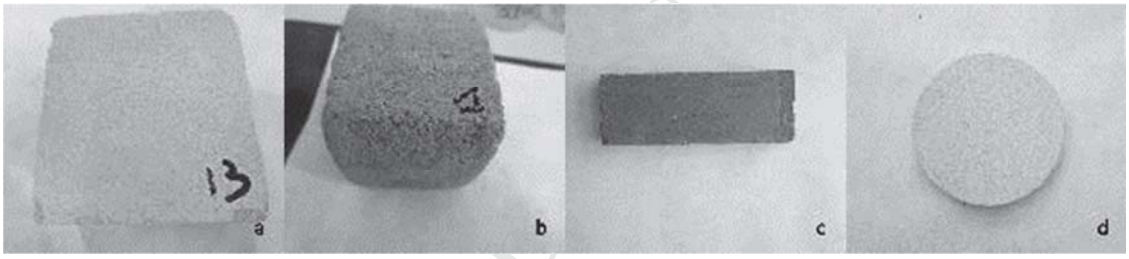

Figure 1. (a) Villamayor Sandstone; (b) Istanbul stone; (c) solid clay brick; (d) lime mortar

The selected substrates were characterized in the following tests:

- Mineralogical analysis by means of X-ray powder diffractometry (XRD), using a Philips X'Pert Pro MPD pw3040/60 copper anode diffractometer, with a 1 h continuous scan from 2 to 75˚ 2Theta, 40kV and 40 mA;
- Petrographic study, according to Standard EN 12407 [17], performed on a thin slice (25x40 mm in size and 30 µm thick of the samples with the aid of a high magnification (x63) binocular loupe and a polarizing microscope with transmitted and reflected light (Nikon Eclipse 6400 POL);
- Porosity, density, average pore size, and pore size distribution were measured with mercury intrusion porosimetry (Autopore IV 9500 from Micromeritics);
- Water absorption at atmospheric pressure, according to Standard EN 13755 [18] and EN 772-21 [19] for clay brick and lime mortar.

2.2 Development and application on selected substrates of two novel IR reflective coatings

Two different coatings were synthetized using two different approaches:

- Coating 1: a silica film synthetized via sol-gel methodology, using silica alcoxide precursors and Indium tin oxide (ITO) nanoparticles. After dissolution in alcohol, these precursors hydrolyse to form silanols [20];

- Coating 2: a water-based solution and/or ethanol solution incorporating ITO in various granularities, with the addition of SiO_2 and TiO_2 in different concentrations and proportions.

2.3Substrate physical-chemical characterization after coatings application

The characterization of the specimens after the coating application consisted of:

- Water absorption at atmospheric pressure, according to the procedure for substrate characterization (Section 2.1);
- Water vapour permeability, determined by the "Cup method" using ISO 788 [21];
- Water contact angle, measured with a Drop Shape Analyzer, as defined in Standard EN 15802 [22];
- Adhesion, assessed by applying and removing pressure-sensitive tape over cuts made in the coating film, as specified in ASTM D3359 [23];
- Solar reflectance by means of a two beam spectrophotometer (from 250 nm to 2500 nm), following ASTM E-903 [24].

2.4 Reversibility and visual impact of the coatings

In addition to substrate compatibility, a further requirement for the surface treatment of historical stone, reversibility, was also tested. Thus, two primers commonly used in cultural heritage conservation, methylcellulose and Paraloid®, were respectively applied at 3% and 15%, before the application of two layers of the two coatings. As colour change is another crucial aspect when restoring heritage structures, colorimetric characterization of the primers and the primer/coating system (i.e., combination of primer and coating) was done before and after application on the different substrates, and after cleaning. The L*, a*, and b* values were measured at three random locations on each specimen with a PCE-TCR 200 colorimeter. After cleaning, the primers were analysed under a Nikon magnifying-glass, while the primer/coating systems were examined with scanning electron microscopy with energy dispersive spectroscopy (SEM/EDS, model FEI Quanta 200).

2.5 Durability tests of the specimens

Durability tests analysed the behaviour of the specimens in the presence of specific agents:

- Salt crystallization;
- Ultra-violet (UV) light;
- Freeze/thaw cycles;
- Wetting/drying cycles.

The resistance of the different substrates to soluble salt crystallization was tested on 44 cubic specimens, each with sides of 40 mm, half treated with coating 1 and half with coating 2, as specified in Standard EN 12370 [25]. Furthermore, two specimens per substrate were exposed to fluorescent UV lamps (UVA-340 model) and water. After 2000 h of ageing with cycles of 4h light and 4h condensation, the final colour was evaluated, following ISO 11507 [26]. A total of 48 cubic specimens with sides of 50 mm were prepared: half were then treated with coating 1 (6 specimens for each substrate type), and the other half with coating 2 (6 specimens for each substrate type), to assess the effect of freeze/thaw cycles. Then, a visual inspection was performed, based on the examination of all faces and edges, to categorize the specimens on the scale in EN 12371 [27]. The test continued until two or more specimens showed "one or several small cracks ($\leq$ 0.1 mm wide) or rupture of small fragments ($\leq$ 30 mm^2) per fragment" (point 3 of the scale reported in the standard). The coated and uncoated samples underwent repeated wetting/drying cycles, to characterize the behaviour of the substrates against thermo-hygrometric variations. 6 cubic specimens with 40-50 mm sides for each substrate were prepared and any visible defect marked, before they were placed in a

HERAEUS HC-0033 damp chamber. The test cycle consisted of 6 h at an air temperature (T_a) of 20 °C and at a relative humidity (RH) of 40%; and then 8 h at a T_a of 60 °C and at a RH of 90%. Upon completion of 5, 12, 19, 26, and 30 wetting-drying cycles, visual inspections confirmed no peeling, flaking, or chipping of a larger average size than 15 mm or cracks in any of the test specimens.

2.6 Thermal performance evaluation of the large scale mock-up wall

Further laboratory tests were designed for sensor measurements on a real-scale mock-up [28] of a traditional brick masonry (1.5 m in width, 1.2 m in height, and 0.48 m in depth) wall. The bricks were manufactured by heating mineral clays in a large "brick kiln" [29; 30; 31]. The wall was constructed using three courses of bricks bonded by a commercial hydraulic lime mortar. Then, a special restoration mortar was applied with a thickness of 0.04 m, both on the inner and the outer surfaces, so that the surface properties were similar to those in the Istanbul case study. The thickness (s) and thermal conductivity (λ-value) values of each material are reported in Table 1.

Table 1. Thickness (s) and thermal conductivity (λ) of the the mock-up wall

Material	s [m]	λ [W/mK]
Brick	0.44	0.47
Hydraulic lime mortar	-	0.83
Restoration mortar	0.04	0.80

The mock-up was kept in the laboratory for approximately 9 months (November 2014 -July 2015), to ensure thermo-hygrometric equilibrium and the uniformity of the internal RH, as required by [32; 33; 34]. After a first run of tests without coating, coating 1 was applied to the exterior surface. The tests were designed to assess: (i) the heat flux reduction with the coating; and, (ii) the outdoor surface temperature, the thermal profile inside the wall and their variation under dynamic conditions. The tests were performed in steady-state and dynamic environmental conditions in a guarded hot box (GHB) with the extra functionality of a lamp field in simulation of the sun (IEC 904-9, class B). European Standard EN 1934 [32] served as a basis to define the sensor distribution. The specimen was surrounded by an EPS insulation frame (from datasheet: $\delta = 250$ kg/m^3; $\lambda = 0{,}033$ W/mK). Two specular regular grids of thermocouples (T-Type built ad hoc, uncertainty (k=2) ± 0.25 °C) were used on the hot and the cold sides to measure the surface temperature difference (ΔT_s) across the specimen. 5 sensors were applied to the monitored areas, 9 in the guarded zone, and 8 in the EPS structure. Furthermore, 9 sensors for T_a monitoring were included both in the hot and the cold chambers to verify the thermal uniformity [32; 33]. Additionally, 8 temperature sensors (Pt 100) were installed on the lateral side of the wall at the maximum depth (0.15 m) to investigate the thermal profile of the specimen: 3 Pt100 sensors distributed equally over the whole depth obtained the overall profile, 4 thermocouples near the hot, exterior side recorded the detailed profile near the irradiated surface, and finally 1 thermocouple supplied measurements for comparison with the innermost Pt100. The heat flux was measured using two cantered HFM plates (Ahlborn type 150-2): (i) one plate mounted between two 3 mm-thick aluminium plates, installed at the interface between the brick wall and the 40 mm layer of restoration mortar under the "outdoor" surface; and, (ii) one plate on the surface of the "indoor" side. The mock-up wall, sensor layout, and the HFM plates are shown in Figure 2.

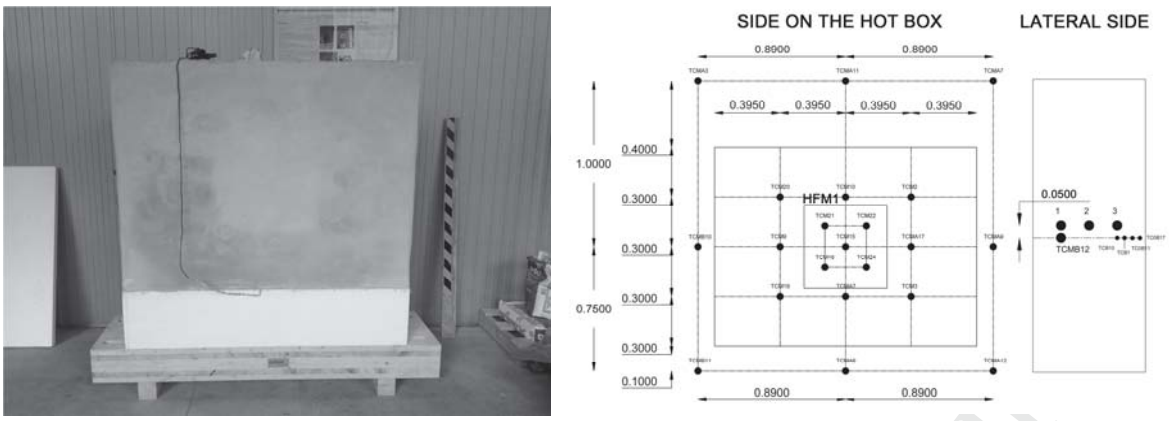

Figure 2. (a) The large scale mock-up of the brick masonry wall with the IR-coating; (b) the sensor layout in the hot chamber and on the lateral side of the wall

Realistic simulation of natural sunlight (BF Engineering, type G-EUR-1107, BBB class) consisted of three main parts: (i) the cabinet with rollers, including the power supply and control system (PLC); (ii) the portable lamp frame (6 daylight lamps Osram HMI 2500 W) on rollers; and, (iii) the reflector tubes to conduct light to the specimen in the climate chamber. A constant T_a of 25 °C was set as an "indoor" condition. The climatic conditions of Seville (data source Meteonorm) were selected as the "outdoor" conditions, representative of the city with the highest radiation in Europe. A typical autumn climate was selected with a 900 W/m² solar radiation peak on a vertical surface (higher than the 500 W/m² peak in summer, for better observation of radiation related phenomena) and a T_a ranging from 20 °C to 30 °C, around an average of 25 °C. This scenario has the advantage that the heat flux due to air temperature differences (ΔT_a) is 0 and the observed heat flux can only be attributed to the radiation effect. Supporting simulations with Delphin 5.8 had shown that the daily average heat flux is the same – whether the wall is exposed to a dynamic temperature (Ta = 25±5 °C sinus wave) and radiation (max 900 W/m²) or to the respective averages (Ta = 25 °C and radiation = 330 W/m²). The average values, were used to determine the heat flux reduction factor with an IR coating compared to uncoated specimens, as it is easier to use "constant" outdoor conditions, while the dynamic measurement was used to study the resulting flux peaks and the temperature distribution within the wall. One further aspect complicated the experimental setup: the artificial sun could only be used in the presence of the lab technician. In a variation to the test conditions at night-time, the outdoor Ta was increased, keeping a constant temperature distribution in the wall while the artificial sun was switched off, so that the mock-up would not cool down. The simulations without the IR coating suggested that a T_s of 30 °C would be reached with the radiation, and of 32 °C without the radiation.

2.7 Thermodynamic simulation of the coating in a reference room

The expected benefits of the IR coating in terms of reduced outside T_s and energy demand under different conditions (climatic zone, surface orientation, ventilation, internal loads) were assessed in a building energy simulation. A building energy model of a typical room (5 x 5 x 3.5 m) was built in EnergyPlus 8.0. software. The model was composed of one vertical surface facing "outside" and another five adiabatic surfaces. Brick walls (s = 0.48 m, λ = 0.47 W/mK resulting in a C-value of 1.2 W/m^{2}K, ρ = 1000 kg/m³, c =1600 J/kgK) were selected for the building envelope. The external facing surface also included a 1.5 x 1.7 m^2 double-glazed window [35]. The following variable parameters were considered: (i) the four main orientations (north, south, east, and west); and, (ii) two climatic locations (Istanbul, Turkey, case study of the project; Seville, Spain, city with the highest solar irradiation in Europe).

Weather data were also simulated with the software Meteonorm [35]. A simulation of IR reflective coating 1 considered average thermal, solar, and visible reflectance values: measured data were weighted averages of each solar wavelength: longwave, shortwave, and visible shortwave spectra, respectively. They were then translated into absorption factors (Table 2) for use in EnergyPlus 8.0 by subtracting the reflectance value from 1 (thermal absorptance (α_t) = 1 – thermal reflectance (τ_t)).

Table 2. Absorptance values used in the building energy simulation - thermal absorptance (α_t), solar absorptance (α_s) and visible absorptance (α_v).

	α_t	α_s	α_v
Brick wall	0.9	0.7	0.7
IR Coated wall	0.79	0.196	0.062

The typical room, designed for the simulation as a residential space, was assigned internal heat gains of 10 W/m² as the base value [36] and 5 W/m² for a scenario of reduced interior loads. The air infiltrations were assumed equal to 0.5 Air Changes per Hour (ACH) (minimum for residential use during occupational hours) [37] and for the scenario with natural ventilation 5 ACH were assumed when the indoor temperature was higher than 24 °C and the outdoor temperature was at least 1 °C lower than indoors. An ideal heating load and cooling system with a constant T_a set point of 20 °C for heating and of 26 °C for cooling [37] was used for the simulation. The following parameters were calculated for the evaluation of the results:

- $\Delta T_{s,\ summer}$: daily temperature cycles in summer calculated as the average daily difference between the maximum and minimum temperatures of the outdoor T_s during summer;
- $T_{s,\ 95,\ summer}$: high temperatures in summer calculated as the 95th percentile of the daily maximum temperatures during summer –corresponding to the 5% highest maxima;
- Heating demand;
- Cooling demand.

2.8 Evaluation under real conditions

The main objective of the Istanbul case study was to test the thermal performance, durability, and reversibility of the new IR reflective coatings on a real historical building. Among the sites available for testing, the city of Istanbul was chosen, due to the climatic conditions, in particular the high solar irradiance. The real historic building selected for evaluation, located in Kallavi Street, Beyoğlu District, is the property of Beyoğlu, one of the oldest districts of Istanbul (Figure 3a). Unfortunately, municipal permits to test the coating directly on the façade were not forthcoming, so samples of different substrates were treated with the new coatings and placed on the roof of the same building at the end of August 2015 (Figure 3b).

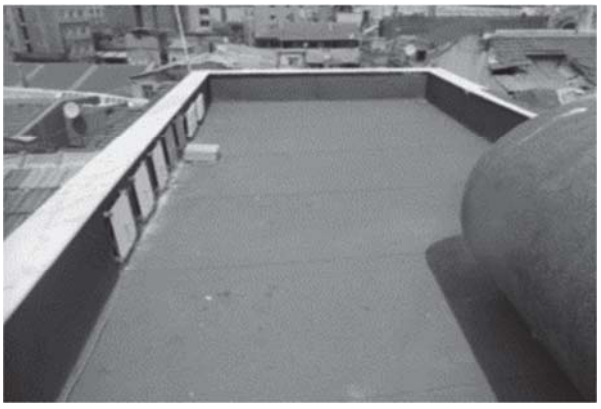

Figure 3. The case study building in Kallavi Street 5, Beyoğlu District, Istanbul: (a) front view of the north façade and (b) aerial view of the roof.

2.8.1 Samples and treatments

8 lime mortar samples 40x40x40 mm and 8 Istanbul stone samples 50x50x30 mm were glued with epoxy resin to 2 timber frames painted white and weather sealed. All the gaps were covered with silicone to avoid water penetration. 5 metal plates 300x300x5 mm were also prepared to evaluate the coatings in accordance with industrial standards.

Coatings 1 and 2 were tested on the different substrates using Paraloid B72 primer, following the results of the previous tests (Section 3.3). The samples of lime mortar and Istanbul stone were treated as follows (Figure 4):

- **R:** 2 reference samples, non-coated;
- **P:** 2 samples painted only with Paraloid B72;
- **S_1:** 2 samples painted with Paraloid B72 and 2 layers of coating 1;
- **S_2**: 2 samples painted with Paraloid B72 and 2 layers of coating 2.

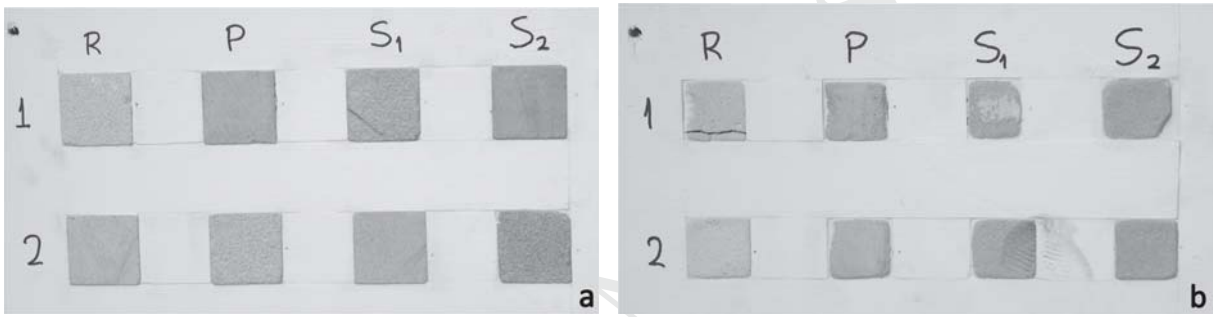

Figure 4. a) Eight lime mortar and b) eight Istanbul stone samples included in timber frames

The metal samples were treated as follows (Figure 5):

- **S_1 white:** white primer, Paraloid B72 and 2 layers of coating 1;
- **S_2 white**: white primer, Paraloid B72 and 2 layers of coating 2;
- **R white:** reference white primer and 1 layer of common varnish (Craft metal) for primer protection;
- **R grey**: reference grey primer and 1 layer of common varnish (Craft metal);
- **S_1 grey**: grey primer, Paraloid B72 and 2 layers of coating 1.

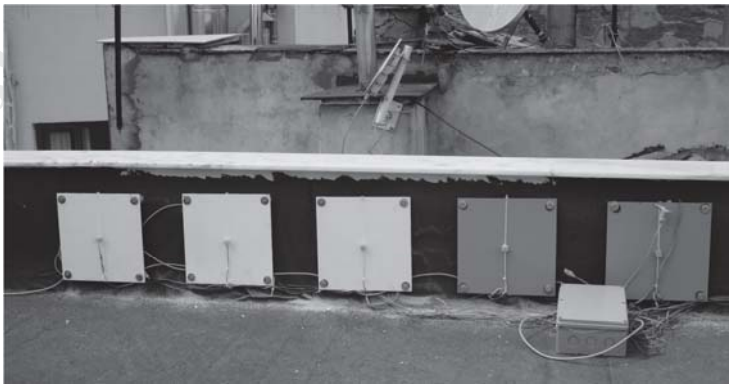

Figure 5. Metal samples

Metal plates and wooden frames were secured to the inner east-facing parapet of the flat roof, in a vertical position, to simulate in every possible way the application to a real historical building.

2.8.2 Monitoring system

The thermal performance of the new reflective coatings was evaluated by comparing the thermal behaviour of both treated and untreated samples of the same substrate. The surface temperature of the samples was measured (within an operating temperature range of -10°C to 30°C with a mean error of ± 0.2°C) with Dallas DS18B20 sensors from Maxim Integrated placed at the back of the samples, protected from direct solar radiation. The thermo-hygrometric conditions (T_a and RH) around the samples were monitored by means of SHT71/75 sensors from Sensirion. A weather station (Vantage Pro2 by Davis) was also installed on a pole located on the roof, to measure air temperature and relative humidity, wind velocity and direction, solar radiation, and precipitation.

The monitoring campaign lasted for about 5 months, from end-August 2015 to mid-January 2016, when the system went down due to a heavy storm. In any case, the data collected were sufficient for the testing of the reflective coatings, as they covered the periods of highest irradiation according to the location and surface orientation (Section 3.5). T_a, RH, and T_s were measured continuously every 10 minutes, the climatic parameters were recorded every 15 minutes. The sensors were connected to the base station placed in a room at the 4th floor of the building. The weather station was equipped with a broadband wireless connection to its console, enabling data transmission over the internet to a server in Italy, and remote access to follow up the system.

The durability of the coatings was assessed by visual SEM inspections before and after 9 months of exposure. Although the monitoring system was down at the beginning of January 2016, the samples exposure lasted until the end of May 2016. The reversibility of the coatings was validated on all the samples through SEM/EDS analysis before and after the removal of the coatings with acetone.

3. RESULTS AND DISCUSSION

3.1 Characterization of the selected substrates

The mineralogical characterization of the Villamayor sandstone consisted of loosely packed quartz and feldspar grains surrounded by clays that also fill intergranular space; the Istanbul limestone consisted of closely packed calcite bioclasts and some intergranular terrigenous clastic sediments; the solid clay brick consisted of quartz grains in a fine-grained reddish amorphous matrix; and finally, the lime mortar consisted of quartz grains in a fine-grained brown calcite matrix (previously portlandite). A porosimetric study also showed the most porous material to be lime mortar (43%), followed by Villamayor sandstone (26.36%), clay brick (18.46%) and lastly the Istanbul limestone (9.92%).

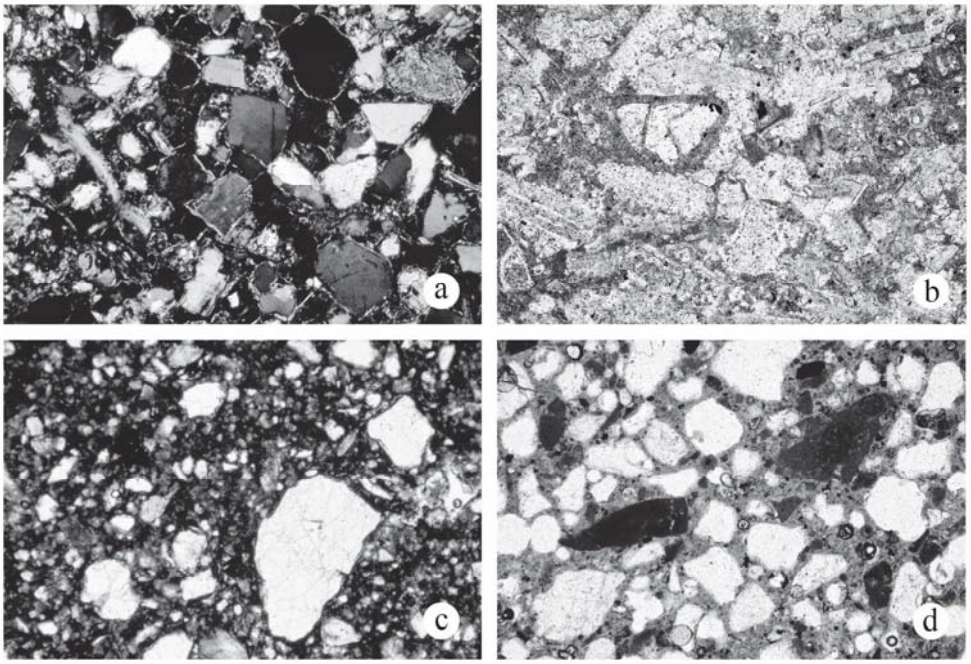

Figure 6. Optical microscopy images of: (a) Villamayor sandstone (field width 2.6 mm); (b) Istanbul limestone (field width 1.3 mm); (c) solid clay brick (field width 2.6 mm); (d) lime mortar (field width 2.6 mm).

3.2 Hygrometric characterization of substrates after the coating application

The average values of the results of water absorption at atmospheric pressure, water-vapour transmission, and hydrophobicity properties are reported in Table 3.

Table 3. Summary characterizations of the substrates after coating application

Property	Parameter	Substrate	Blank	Coating 1	Coating 2
Absorption at atmospheric pressure	Absorption (%)	Villamayor sandstone	15	3	8
		Istanbul stone	3	1	1
		Solid clay brick	7	7	7
		Lime mortar	8	2	2
Water vapour permeability	Water vapour transmission rate ($g/m^2.d$)	Villamayor sandstone	211.40	160.09	129.36
		Istanbul stone	8.28	7.66	8.11
		Solid clay brick	29.90	23.70	17.31
		Lime mortar	119.30	91.07	70.73
Hydrophobicity	Water contact angle (º)	Villamayor sandstone	0	115.08	76.90
		Istanbul stone	0	85.38	68.56
		Solid clay brick	0	88.01	72.08
		Lime mortar	23.55	115.50	73.35
Solar radiation	Reflectance (%)	Villamayor sandstone	50	61	63
		Istanbul stone	66	75	77
		Solid clay brick	45	55	56
		Lime mortar	64	75	77

In the case of the Villamayor sandstone, coating 1 was more effective at reducing atmospheric moisture absorption (80%) than coating 2 (47%). Absorption on both coatings over the Istanbul limestone was reduced by approximately 33%. The coatings on the solid clay brick hardly varied from their initial behaviour in terms of water absorption. Absorption on lime mortar with both coatings was reduced by 75%. According to the results, the coatings were more effective on the sandstone and had little or no effects on the ceramic bricks. The water absorption capacity of both the Istanbul limestone and the lime mortar were reduced. By applying the coating, water vapour transmission was reduced in all cases. By using coating 1, the value for all the specimens, except for the Istanbul stone, was reduced by about 20%, while the application of coating 2 reduced the value by about a 40%. Coating 2 reduced the water vapour absorption (2% against 7% registered by coating 1) less than coating 1 on the Istanbul limestone, however it must be noted that the value was also very low for the blank specimen. The test results, in this case, indicate a preference for coating 1 rather than coating 2. Both coatings also improved the hydrophobic properties of the substrates. Water repellence was improved most of all on the Villamayor sandstone and on the lime mortar, especially with coating 1 where hydrophobicity was around 35% higher than coating 2. The properties of the Istanbul stone and the solid clay brick were improved and coating 1 provided 20% higher water repellence compared to coating 2. Regarding the solar radiation properties, the NIR spectra of the coatings applied on the different substrates showed average differences of 10% compared to the untreated substrates, clearly demonstrating the reflective properties of the coatings.

3.3 Reversibility and visual impact of the coatings

An ideal coating should not change the visual appearance of the surface to which it is applied and should not undergo degradation over time. Typically, a colour difference (ΔE^*) value of under 3 units is not perceptible to the human eye [39]. However, in the field of conservation, a total colour difference of up to 5 units after the application of a surface treatment is generally considered acceptable [39]; the latter value was considered a threshold value during the evaluation of the coatings in terms of both the visual blend with the substrate and reversibility.

The results associated with the primer characterization showed notable colour changes associated with Paraloid primer on 2 of the 4 substrates under analysis, i.e. Villamayor sandstone and Istanbul stone, while the test results with the methylcellulose primer were within acceptable ranges for all the substrates (Figure 7). The testing of the primer/coating systems showed that the total colour variation was higher than 5 units for:

- Villamayor Sandstone following application of both primers and coating 2 (M2 and P2);
- Villamayor Sandstone and Istanbul stone following application of the Paraloid primer and coating 1 (P1);

All these combinations were reversible after cleaning until no colour change was apparent (Figure 7). Coating 2 applied to the solid clay brick with either methylcellulose or Paraloid, showed a colour change of up to 5 units, with a slight increase after cleaning. The results indicated that, in general, coating 2 had greater visual impact than coating 1.

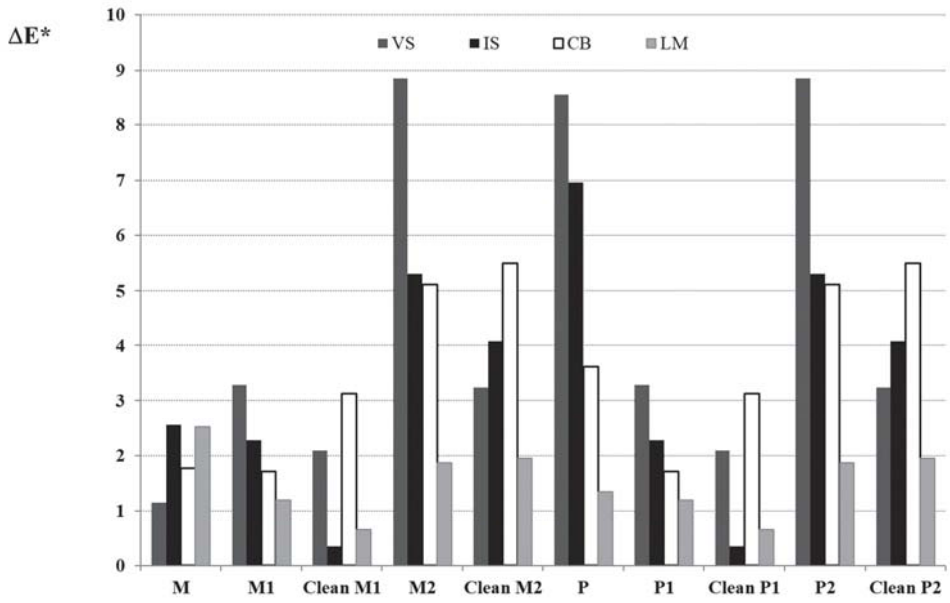

Figure 7. Total colour variations of the different substrates (Villamayor Sandstone VS, Istanbul Sandstone IS, Clay brick CB, Lime Mortar LM) after application of primers (Methylcellulose M and Paraloid B72 P), after treatment with primer/coating systems 1 (M1, P1) and 2 (M2, P2), and after cleaning (Clean M1, Clean M2, Clean P1, Clean P2)

SEM and EDS analyses verified the reversibility of the coatings, comparing the samples before and after the treatment. Firstly, the main elements of each substrate were analysed and the elements of the aforementioned coatings, secondly a detailed analysis of the SEM and the EDS images was conducted. The results are summarized in Table 4.

Table 4. Reversibility of the primer and the primer + coatings on the substrates

SUBSTRATE	PRIMER	REVERSIBLE	COATING	REVERSIBLE
		Nikon Magnifying -glass		SEM
Villamayor sandstone	Paraloid	√	Coating 1	√
			Coating 2	√
	Methylcellulose	√	Coating 1	√
			Coating 2	**X**
Clay brick	Paraloid	√	Coating 1	√
			Coating 2	√
	Methylcellulose	√	Coating 1	X
			Coating 2	**X**
Lime mortar	Paraloid	√	Coating 1	√
			Coating 2	√
	Methylcellulose	X	Coating 1	X
			Coating 2	X
Istanbul stone	Paraloid	√	Coating 1	√
			Coating 2	√

	Methylcellulose	√	Coating 1	X
			Coating 2	X

According to the SEM images and colorimetric results, Paraloid was selected as the most suitable primer to ensure the reversibility of the coating, and consequently it was used in the Istanbul case study.

3.4 Durability tests of the specimens

3.4.1 Salt crystallisation

Salt crystallization tests were performed to determine the durability of the different substrates impregnated with both coatings and their resistance. The specimens experienced notable degradation when submitted to repeated cycles of salt crystallization, to an extent directly proportional to the porosity of the material. In the case of the Villamayor sandstone, all the samples collapsed before the end of the test of 15 cycles. All the specimens of Istanbul limestone at the end of the test showed the same mass with coatings 1 and 2, while only 1 specimen of clay brick was degraded. The lime mortar specimens treated with coating 1 were visibly damaged at an earlier stage of testing than those treated with coating 2; the specimens treated with coating 2 showed no signs of damage almost up until the last few cycles.

3.4.2 UV Tests

The results of the UV ageing test for both coatings are shown in Figure 8. The measurements taken on 2 specimens per substrate were averaged. For all the substrates, the total colour variation after UV exposure was below the threshold of 5 units that is generally acceptable in the field of cultural heritage [39].

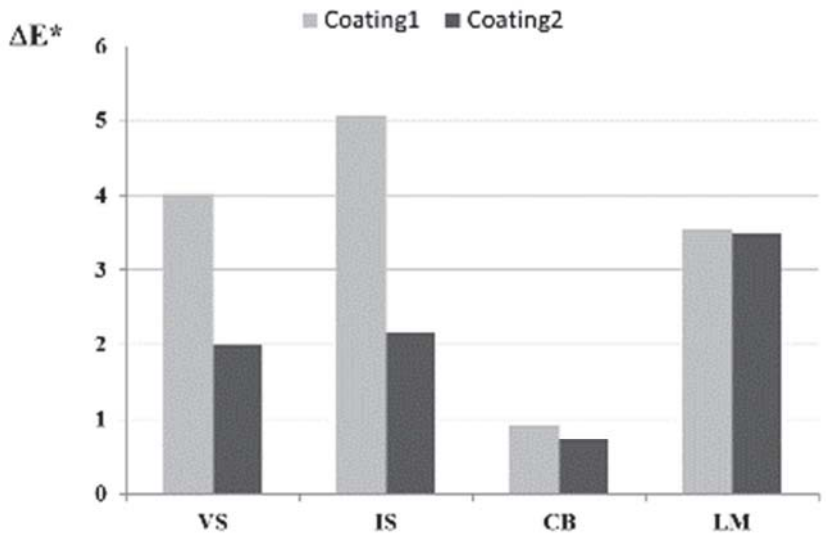

Figure 8. Total colour variations observed in the different substrates (Villamayor Sandstone VS, Istanbul Sandstone IS, Clay brick CB, Lime Mortar LM) treated with coating 1 and coating 2 after UV ageing

3.4.3 Freezing/thawing tests

The evaluation of the freeze/thaw effect was done by visual inspection. All specimens resisted repeated cycles, except the solid clay bricks. In the case of the Villamayor samples, after 15 cycles, damage, from minimal damage to several cracks, was detected in the specimens treated with coating 1, while specimens treated with coating 2 resisted up to 35 cycles before showing minimal damage in 2 specimens and several cracks in the other 4. The Istanbul

limestone specimens, regardless of the type of treatment (coating 1 or 2), resisted 90 cycles, showing small cracks and little loss of material. For lime mortar, specimens treated with coating 1 showed better behaviour than the ones treated with coating 2, as the same range of damage occurred with a lower number of cycles. In the case of brick, severe damage was detected after only 5 cycles, again regardless of treatment. The lime mortar specimens, characterised by high porosity and large pore size, behaved better than the sandstone specimens, also of high porosity but of smaller pore size, showing damage after 44 and 35 cycles, respectively with coating 1 and 2. The material with the best performance was limestone, characterized by its low porosity, small pore size and low water absorption values while the solid clay brick showed the worst performance against frost.

3.4.4 Wetting/drying cycles

No relevant damage was observed in the materials under analysis after 30 wetting and drying cycles (Figure 9). Colour change was imperceptible to the human eye following the application of coating 1 on both sandstone and limestone, and in only 1 specimen was colour change perceptible, but still acceptable (section 3.3). No colour change in all the specimens was perceptible to the human eye after the application of coating 2, in all the specimens. No colour change was perceptible on the brick with either coating. In the case of lime mortar, coating 1 produced an acceptable change in 1 specimen while coating 2 produced no colour change. Therefore, no colour changes were generally associated with coating 2 in almost all the specimens under analysis.

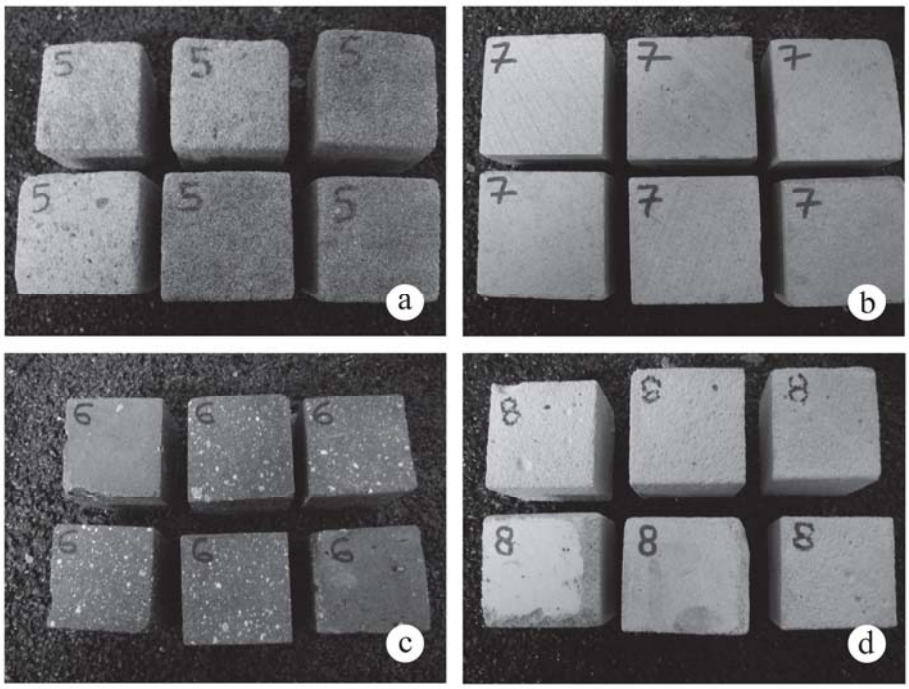

Figure 9. Specimens after 30 wetting/drying cycles: (a) Villamayor sandstone; (b) Istanbul limestone; (c) Solid clay brick; (d) Lime mortar

3.5 Thermal performance evaluation of the large scale mock-up wall

Results of the steady state measurements showed a flow into the wall of 11 W/m² (without coating) and 8.5 W/m² (with coating). Therefore, the presence of the coating reduced the heat flow by 2.5 W/m² compared to the situation without coating, equal to a 23 % reduction. Assuming an absorption factor of the wall without coating ($\alpha_{w/o}$) of 0.6, this difference would result in an absorption factor for the coated wall (α_{with}) of 0.46:

$$\alpha_{with} = \frac{I_{abs,with}}{I_{bb}} \quad with \quad I_{bb} = \frac{I_{abs,w/o}}{\alpha_{w/o}} \quad therefore \quad \alpha_{with} = \frac{I_{abs,with}}{I_{abs,w/o}} \alpha_{w/o} = \frac{8.5}{11} \, 0.6 = 0.46$$

$\alpha_{w/o}$ = absorption factor, wall without coating
α_{with} = absorption factor, wall with coating
I_{bb} = radiation absorbed by a black body
$I_{abs,\ w/o}$ = absorbed radiation, without coating
$I_{abs,\ with}$ = absorbed radiation, with coating

The thermal profile within the wall during the dynamic test shows how the temperature increased with the irradiation and decreased during night (Figure 10). This phenomenon was less pronounced with increasing depth: in fact, the difference between the highest and lowest values was respectively 13.1 °C in P1 (depth of 0.03 m) and 6.1 °C in P3 (0.12 m), while in P5 (0.36 m) the temperature remained practically constant. At a certain point, the temperature profile was inverted: the outer layers cooled down faster, while temperatures were still higher deeper in the wall. The phenomenon was similar for the coated wall, but the temperature increase due to irradiation was lower (Table 5). The respective heat flux peaks measured every day and every night were high with respect to the average flux. The 24 h average of the flux measured with the HFM at 0.04 m below the outside surface corresponded to the rather constant heat flux at the interior surface. The dynamic measurements indicated a maximum heat flow of around 105 W/m² in the original wall and 81 W/m² for the wall with the IR coating, the same percentage reduction as in the steady state test.

Table 5. Temperature profile within the wall during dynamic tests without and WITH coating

		Temperature without coating (°C)			Temperature WITH coating (°C)		
		max	min	delta	max	Min	delta
P0	3 cm	37.5	24.4	13.1	34	23.5	10.5
P3	12 cm	32.8	26.7	6.1	29.7	24.5	5.2
P5	36 cm	n.a.	n.a.		26.1	25	1.1

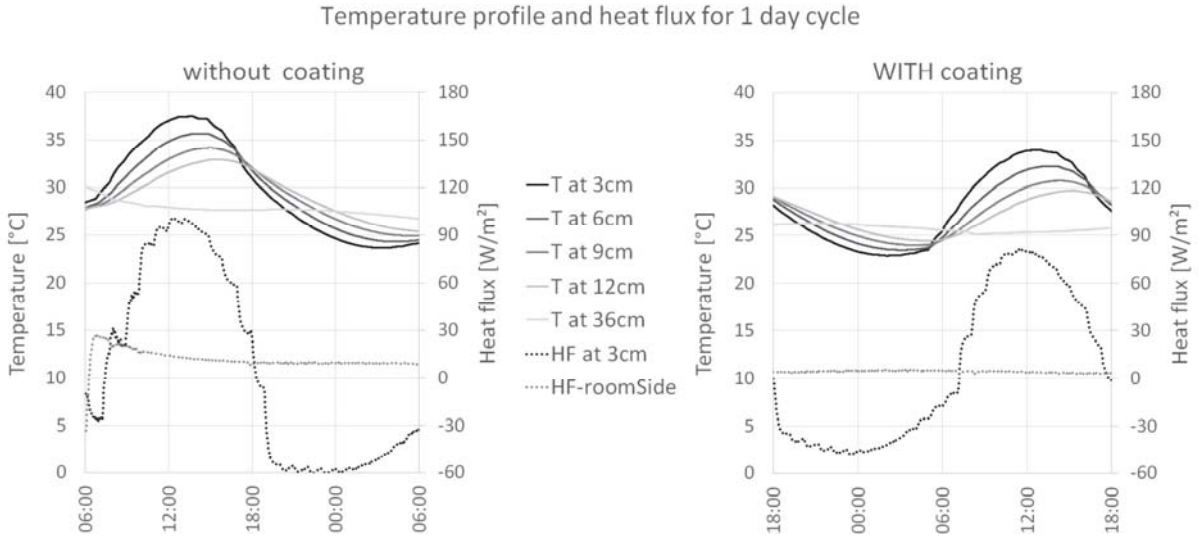

Figure 10. Results of the dynamic test without (a) and with (b) the IR coating

The estimation of the measured absorption coefficient at around 0.46 is a characteristic of the coating itself, while the reduction of the energy flow by 23 % is specific for this boundary condition (e.g. interior and exterior air temperature of 25 °C, see Section 2.6).

3.6 Thermodynamic simulation of the coating in a reference room

The building energy simulations were done in different climate scenarios, as cited in Section 2.7, to understand the benefits of the IR coating over the whole year, both in terms of reducing the outdoor T_s, its daily cycle and the energy demand [35]. A clear benefit could be shown for the reduction of the outdoor T_s and consequently the reduction of surface thermal stress. The average daily thermal variation in the Istanbul climate (IST) of T_s in summer was reduced from about 15 °C to less than 7 °C. The "summer high temperatures" $T_{s,95,summer}$ descended from over 40 °C to around 30 °C (Figure 11). In Seville's climate (SEV) the effect was even more pronounced: the daily temperature cycles were reduced from more than 20 °C to around 10 °C and the high maxima $T_{s,95,summer}$ descended from 50 °C to 35-40 °C. In both cases, the effects of the IR coating were less pronounced for the north wall, but very similar for all other direction – with one exception: as the eastern orientation in Seville was characterized by the highest T_s and cycles, the benefit with the coating was at its highest.

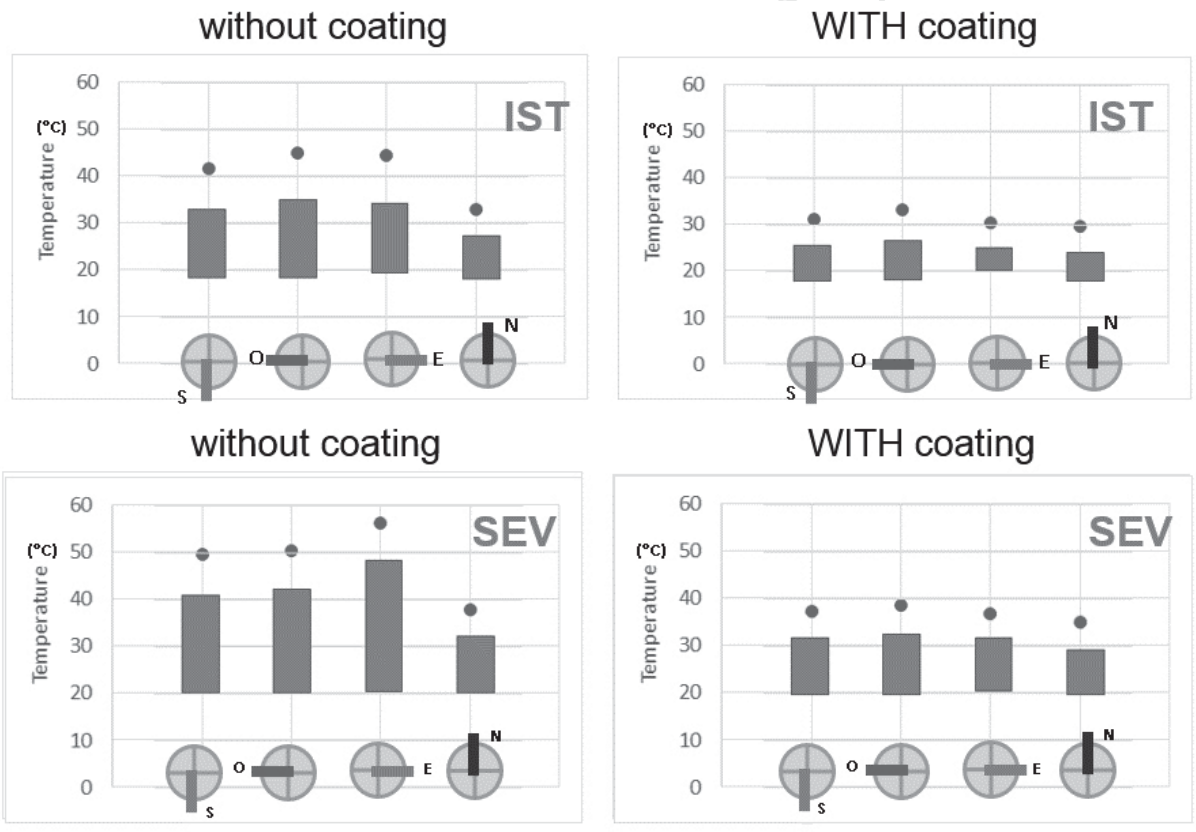

Figure 11. Effect of the IR coating on the outdoor T_s. in terms of 5% highest daily maxima (dots) and daily thermal cycles (bars). The height of the bar shows the actual surface temperature (°C), its position the actual average minimum and the maximum temperatures for the four orientations in Istanbul (IST) and Seville (SEV) climates. The bars in the circles show the orientation of the facades whit the coating (N = north, S = south; E = east; O = west).

The improvements in energy performance, heating and cooling demand over the whole year were calculated, for the assessment of the second expected benefit of the IR coating. In Seville, the cooling demand in the base scenario was reduced by the IR coating from about 67.4 to 60.0 kWh/m² (-7.4 kWh/m²), while the heating demand was too small to matter (in the model room and conditions). In Istanbul, the cooling demand in the base scenario was

reduced from 42.8 to 37.5 kWh/m² (-5.3 kWh/m²), although that reduction was partly counterbalanced by a heating demand increase from 13.2 to 15.8 kWh/m² (+2.6 kWh/m²). Finally, other "summer case optimization strategies" such as reducing interior loads and natural ventilation strategies were analysed. The scenario "natural ventilation" (as described in section 2.7), led to a cooling demand reduction in Istanbul from 42.8 to 19 kWh/m² (without coating) and from 37.5 to 17 kWh/m² (with the coating); a reduction of over 50%. Similarly, the "reduced load" scenario in the Istanbul climate led to a reduction from 42.8 to 24.2 kWh/m² (without coating) and from 37.5 to 19.9 kWh/m² (with coating).

3.7 Evaluation under real conditions

The climate in Istanbul is 'Mediterranean' (Köppen Climate Classification: 'Csa'), with very warm summers and relatively mild winters. Measurements collected in Istanbul as well as data generated as a test reference year indicated that the daily average total solar radiation on a horizontal surface is highest in June-July, with maxima reached between 12:00-13:00 h [40; 41]. As the samples under study were placed in a vertical position and oriented towards the east, the lighting design software DIALux was used to estimate the impact of solar radiation on them throughout the year, to identify the most significant periods for the evaluation of the performance of the coatings. According to the results, the highest intensity of solar radiation in the case study location (Kallavi Sk., 34430 Beyoğlu, Istanbul; 41°01'56.9"N 28°58'32.7"E) for a vertical east-facing surface is reached around the autumn equinox. Moreover, the detailed analysis of the hourly solar radiation trends in that period show that solar radiation increases from about 6:30 (sunrise) till 10:30, when it reaches its maximum; hence the data analysis was focused on that temporal window.

The analysis of the front surface temperatures of the metal samples showed that both the average and highest T_s values of the treated specimens were generally of a few tenth lower than the reference specimen (Table 8), indicating that the reduction of the surface thermal stress due to the presence of the reflective coatings was very small.

Table 8. Average and highest values of T_s measured at the front of the metal samples without and with coating

Sample ID	S1 Grey	R Grey	S1 White	S2 White	R White
Colour	Grey	Grey	White	White	White
Coating	1	None	1	2	None
T Average (°C)	29.9	30.0	26.8	26.5	26.9
T Maximum (°C)	50.6	50.3	41.1	40.6	41.4

The back surface of the treated samples was characterized by T_s equal or lower than the reference sample T_s for at least half of the monitoring period and time considered (46% for S1 grey, 76% for S1 white, 69% for S2 white). Moreover, the highest thermal values of the back surfaces were reduced as well (of 4.7°C for S1 grey, 7.8°C for S1 white, 8.0°C for S2 white), while average T_s showed notable reductions only for S1 white (i.e., of 0.5°C). These results indicated that the combination of a white substrate and coating 1 was the most effective. In the case of Istanbul stone, only the back surface of the exposed samples was monitored, but in addition the thermal behaviour of the primer was investigated. The results showed the following general trend in the period and the hours selected for analysis: $R > P \geq S2 > S1$ (Figure 12).

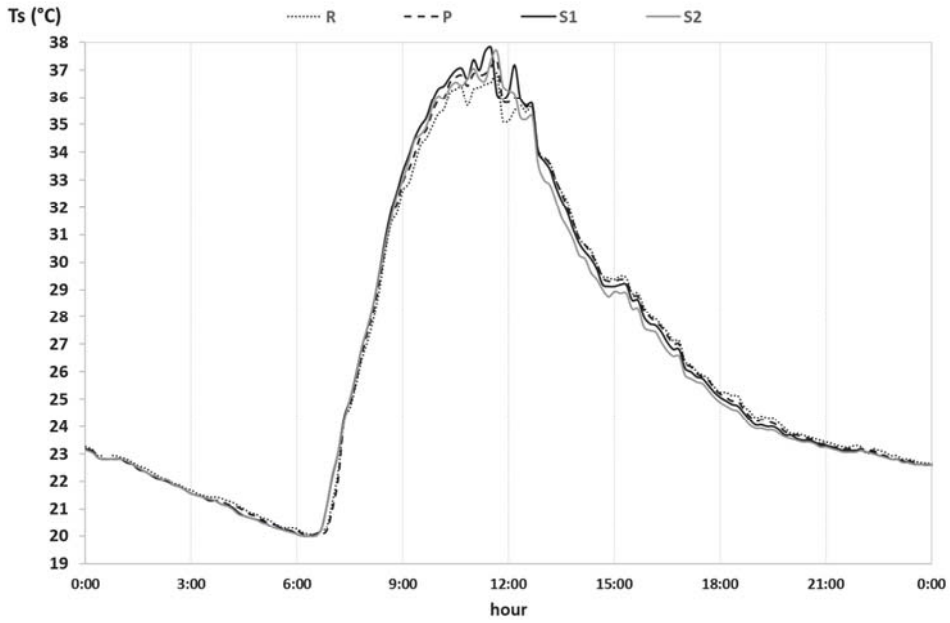

Figure 12. Hourly trend of the temperatures recorded on the back surfaces of the Istanbul stone samples in late September. S1: coating 1+Paraloid; S2: coating 2+Paraloid; P: Paraloid; R: reference (untreated).

Moreover, the statistical data analysis indicated that for over half of both the monitoring period and the temporal window, the back T_s of the treated sample was lower or comparable to the T_s of the untreated sample, regardless of the treatment type. The average values of the differences between the T_s of the differently treated samples and the reference ones were then calculated: R-S1=0.4 °C; R-S2=0.2 °C; R-P=0.2 °C. Taking into account sensor accuracy and the error propagation rules, that difference was more significant for samples treated with the Paraloid + coating 1 system (S1), while the samples treated with the Paraloid + coating 2 system (S2) showed a similar thermal behaviour to the samples treated only with primer (P). The same kind of analysis was also performed on data collected on mortar samples, indicating a behaviour very similar to Istanbul stones, as the back T_s of the treated samples over most of the time-period under study was lower than the untreated sample, once again regardless of treatment. In any case, the average difference between the T_s of the differently treated samples and the reference sample was not so remarkable: on average 0.3 °C for samples S1 and S2, and 0.2°C for sample P.

Regarding durability, after 9 months (M9) of exposure any sign of deterioration was visually observed on the samples. Moreover, the SEM micrographs taken at M9 indicated that the coatings were not damaged after 9 months of exposure. The SEM images of surface topography of all the samples before and after coating removal were analysed following the same procedure described in Section 3.3. In the case of the metal plates, the target was to remove the transparent coatings, but not the white/grey primers. The results are summarized in Table 9.

Table 9. Reversibility of coating on the substrates

SUBSTRATE	COATING	REVERSIBLE SEM
Metal plate	1 white	√
	2 white	X
	1 grey	√
Lime mortar	Paraloid	√

	1	√
	2	√
Istanbul stone	Paraloid	√
	1	√
	2	X

In conclusion, all coatings, except coating 2, were removed completely. Coating 2 would probably have been completely removed with a second cleaning.

4. CONCLUSIONS

Two new IR reflective coatings have been investigated as possible solutions that can improve the thermal performance of historic buildings through an extensive study that has included: laboratory analyses of treated specimens, tests in a large scale mock-up of a traditional masonry structure, thermodynamic simulations, and finally evaluation on a real historic building in the centre of Istanbul. Two different coatings compatible with historic materials were developed and applied to 4 selected substrates commonly used in European cultural heritage, i.e., Villamayor Sandstone, Istanbul stone (the same of the case study), solid clay bricks, and lime mortar.

The results of the laboratory analyses indicated that the application of both coatings reduced atmospheric moisture absorption of the specimens and improved their hydrophobic properties, however water vapour transmission was only slightly reduced. The use of a Paraloid primer prior to the coating application guaranteed its reversibility and was verified by SEM analysis. Due to the porosity of the selected substrates, the specimens experienced notable decay when subjected to salt crystallization tests despite their coatings. All the materials in the analysis showed no relevant damage following wetting and drying cycles and presented acceptable values in ageing tests.

Laboratory testing of coating 1 on the mock-up wall in combination with the thermodynamic simulations in EnergyPlus showed that during both winter and summer the coating stabilized the external surface temperature of the wall, reducing mechanical stress, and consequently extending the life of the structure. The results are more difficult to generalize in terms of energy benefits related to reductions in the heat absorbed by the wall. The simulation in a small reference room ($A = 5x5m^2$) showed that cooling demand reduction in summer might be counterbalanced by increased heating demand in winter. The combination of the application of the IR coating with other actions have shown themselves to be more effective and might be the best option, especially where the possibilities for ventilation and load reduction are limited. Two clear “opportunity cases” for the application of the IR coating can be identified in this case: (i) hot climates, where no heating is needed and no drawback in winter has to be considered; and, (ii) warm climates, where the IR coating reduces the cooling needs, and is especially useful when no cooling system has been installed (saving on investment in the system and installation in the building).

The reflective property of the coatings, i.e., the reduction of thermal stress on the surfaces, could not be clearly proven during the tests on a real historic building, probably due to the experimental set-up and, in particular to the small size of the coated areas. However, the coatings showed durability and reversibility properties after exposure to an outdoor climate.

Several commercial products are available in the market with energy saving properties, e.g., Gaina, Nanopinturas®, Thermo-shield® exterior wall, and Nansulate® Crystal. Besides their reflective properties, these products will in general produce colour changes and will only be removable with intrusive cleaning techniques, which can damage the substrate in an irreversible way.

A huge effort within EFFESUS has moved this work beyond the state of the art, to develop an effective product with many simultaneous benefits. Besides the reflection potential, the properties of hydrophobicity, transparency, reversibility, and physico-chemical compatibility with a variety of historic substrates are the unique advantages of these innovative IR coatings. As the coating formulations contain TiO_2 nanoparticles (coating 2) or can include others (coating 1), further studies are in progress in order to prove their anti-moulding, anti-bacterial and anti-pollutant properties, which will increase their potential competitiveness, adding positive advantages for any future retail commercialization.

ACKNOWLEDGEMENTS

The EFFESUS project has received funding from the European Union Seventh Framework Programme for research, technological development and demonstration under grant agreement No. 314678. The authors are grateful to Arianna Vivarelli for her contribution to the activities of the project.

BIBLIOGRAPHY

1 A. L. Pisello, State of the art on the development of cool coatings for buildings and cities, Solar Energy 144 (2017) 660-680.

2 A. Santamouris, T. Synnefa, Karlessi, Using advanced cool materials in the urban built environment to mitigate heat islands and improve thermal comfort conditions, Solar Energy 85 (2011) 3085-3102.

3 P. Berdahl, S.E. Bretz, Preliminary survey of the solar reflectance of cool roofing materials, Energy and Building 25 (1997) 149-158.

4 A. Rosenfeld H. Hashem Akbari, S. Bretz, B. L. Fishman, D. M. Kurn, D. Sailor, H. Taha, Mitigation of urban heat islands: materials, utility programs, updates, Energy and Buildings 22 (1995) 255-265.

5 C. Ferrari, A. Muscio, C. Siligardi, Effect of aging processes on solar reflectivity of clay roof tiles, Adv. Build. Energy Res. 8 (2014) 28-40.

6 H. Shen, T. Hongwei, A. Tzempelikos, The Effect of Reflective Coatings on Building Surface Temperatures, Indoor Environment and Energy consumption. An Experimental Study, Energy and Buildings 43 (2011) 573-80.

7 A. Synnefa, M. Santamouris, I. Livada, A Study of the Thermal Performance of Reflective Coatings for the Urban Environment, Solar Energy 80 (2006) 968-981.

8 X. Wang, C. Kendrick, R. Ogden, J. Maxted, Dynamic Thermal Simulation of a Retail Shed with Solar Reflective Coatings, Applied Thermal Engineering 28 (2008) 1066-1073.

9 A. Synnefa, M. Santamouris, H. Akbari, Estimating the Effect of Using Cool Coatings on Energy Loads and Thermal Comfort in Residential Buildings in Various Climatic Conditions, Energy and Buildings 39 (2007) 1167-1174.

10 P. Berdahl, Building Energy Efficiency and Fire Safety Aspects of Reflective Coatings, Energy and Buildings 22 (1995), 187-191.

11 A. L. Pisello, F. Cotana, The Thermal Effect of an Innovative Cool Roof on Residential Buildings in Italy: Results from Two Years of Continuous Monitoring, Energy and Buildings 69 (2014) 154-164.

12 A. Joudi, H. Svedung, M. Cehlin, M. Rönnelid, Reflective Coatings for Interior and Exterior of Buildings and Improving Thermal Performance, Applied Energy 103 (2013) 562-570.

13 M. Santamouris, D. Kolokotsa, On the impact of urban overheating and extreme climatic conditions on housing, energy, comfort and environmental quality of vulnerable population in Europe, Energy Buildings 98 (2015) 125-133.

14 F. Cotana, F. Rossi, M. Filipponi, V. Coccia, A. L. Pisello, E. Bonamente, A. Petrozzi, G. Cavalaglio, Albedo control as an effective strategy to tackle Global Warming: A case study, Applied Energy 130 (2014) 641-647..
15 EFFESUS Project, http://www.effesus.eu (accessed 3.8.2016).
16 E. Lucchi, F. Becherini, M. C. Di Tuccio, A. Troi, J. Frick, F. Roberti, C. Hermann, I. Fairnington, G. Mezzasalma, L. Pockelé, A. Bernardi, Thermal performance evaluation and comfort assessment of advanced aerogel as blown-in insulation for historic buildings, Building and Environment 122 (2017) 258-268.
17 AENOR (Asociación Española de Normalización y Certificación), Natural stone test methods. Petrographic examination, Standard UNE-EN 12407, 2001.
18 AENOR (Asociación Española de Normalización y Certificación), Natural stone test methods. Determination of water absorption at atmospheric pressure, Standard UNE-EN 13755, 2008.
19 AENOR (Asociación Española de Normalización y Certificación), Methods of test for masonry units. Part 21: Determination of water absorption of clay and calcium silicate masonry units by cold water absorption, Standard UNE-EN 772-21, 2011.
20 A. V. Rao, S. S. Latthe, D. Y. Nadargi, H. Hirashima, V. Ganesan., Preparation of MTMS based transparent superhydrophobic silica films by sol–gel method, Journal of Colloid and Interface Science 332 (2009) 484-490.
21 ISO (International Organization for Standardization), Paints and varnishes. Determination of water-vapour transmission properties. Cup method, Standard ISO 7783, 2011.
22 AENOR (Asociación Española de Normalización y Certificación), Conservation of cultural property - Test methods - Determination of static contact angle, Standard UNE-EN 15802, 2010.
23 ASTM International (American Society for Testing and Materials), Standard Test Methods for Measuring Adhesion by Tape Test, Standard ASTM D3359, 2009.
24 ASTM International (American Society for Testing and Materials), Standard Test Method for Solar Absorptance, Reflectance, and Transmittance of Materials Using Integrating Spheres, Standard ASTM E903, 2012.
25 AENOR (Asociación Española de Normalización y Certificación), Natural stone test methods. Determination of resistance to salt crystallisation, Standard UNE-EN 12370, 1999.
26 ISO (International Organization for Standardization), Paints and varnishes. Exposure of coatings to artificial weathering. Exposure to fluorescent UV lamps and water, Standard ISO 11507, 2007.
27 AENOR (Asociación Española de Normalización y Certificación), Natural stone test methods. Determination of frost resistance, Standard UNE-EN 12371, 2011.
28 A. Troi, L. Baglivo, E. Lucchi, F. Roberti, Novel measurement approach to determine the energetic performance of an IR reflective coating on a historic wall in the lab, EURAC report, 2017.
29 S. Adhikari, E. Lucchi, V. Pracchi, Experimental Measurements on Thermal Transmittance of the Opaque Vertical Walls in the Historical Buildings, in J. Reiser, C. Jiménez, S. Biondi Antúnez de Mayolo (eds.), Proceedings of the 28th International PLEA Conference on Sustainable Architecture & Urban Design: Opportunities, Limits and Needs. Towards an Environmentally Responsible Architecture, PLEA 2012, Lima, 7-9 November 2012.
30 E. Lucchi, Non-invasive method for investigating energy and environmental performances in existing buildings, in AA. VV. (eds.), Proceedings of the 27th International PLEA Conference on Passive and Low Energy Architecture, PLEA 2011 “Architecture and Sustainable Development”, Louvain-la-Neuve, 13-15 July 2011, pp. 571-576.
31 Lucchi, E., Tabak, M., Troi, A., The "cost Optimality" Approach for the Internal Insulation of Historic Buildings, Energy Procedia, 133 (2017) 412-423.

32 UNI (Ente Nazionale Italiano di Unificazione), Prestazione termica degli edifici. Determinazione della resistenza termica per mezzo del metodo della camera calda con termoflussimetro, Standard UNI EN 1934, 2000.
33 ASTM International (American Society for Testing and Materials), Standard Test Method for Thermal Performance of Building Materials and Envelope Assemblies by Means of a Hot Box Apparatus, Designation C1363, 2011.
34 ISO (International Organization for Standardization), Thermal Insulation. Determination of the Steady-state Thermal Transmission Proprieties. Calibrated and Guarded Hot Box, Standard ISO 8990, 1994.
35 F. Roberti, E. Lucchi, A. Troi, Effects of Radiation Reflective Coatings Applied to Massive Walls, in AA. VV. (eds.), Proceedings of the 31st International PLEA Conference on Passive and Low Energy Architecture, PLEA 2015 "Building Green Futures", Bologna, 8-11 September 2015.
36 ASHRAE (American Society of Heating, Refrigerating, and Air-Conditioning Engineers), ASHRAE Fundamentals, Cap. 10, ASHRAE, Atlanta, 2013.
37 CEN (European Committee for Standardization), Criteri per la progettazione dell'ambiente interno e per la valutazione della prestazione energetica degli edifici, in relazione alla qualità dell'aria interna, all'ambiente termico, all'illuminazione e all'acustica, Standard EN 15251, 2008.
38 R. M. Esbert, J. Ordaz Gargallo, F. J. Alonso Rodríguez, M. Montoto San Miguel, T. González Limón, M. Álvarez de Buergo, Manual de diagnosis y tratamiento de materiales pétreos y cerámicos. Colẽgi d'Aparelladors i Arquitectes Tècnics de Barcelona, 1997.
39 J. Delgado Rodrigues, A. Grossi, Indicators and ratings for the compatibility assessment of conservation actions, Journal of Cultural heritage 8 (2007) 32-43.
40 S. Topcu, S. Dilmac, Z. Aslan, Study of hourly solar radiation data in Istanbul, Renewable Energy 6, 2 (1995) 171-174.
41 H. Bulut, Generation of typical solar radiation data for Istanbul, Turkey, International Journal Energy Res, 27 (2003) 847-855.

Highlights

- Development of IR reflective coatings compatible with historic substrates in the framework of the EC Project EFFESUS
- Physical-chemical characterization, reversibility, aesthetic impact and durability tests
- Thermal performance assessment on a large scale mock-up and thermodynamic simulation
- Evaluation of thermal performance, durability and reversibility in a historic building in Istanbul
- Improved substrate atmospheric moisture absorption, hydrophobicity and durability of the material
- Reduction of mechanical stress and lifetime extension of the structure
- Main advantages for application in historic buildings: transparency, physico-chemical compatibility, reversibility